

4WD Electric Vehicle Battery Test Candidate Under Several Speeds Topologies Variations for Utility EV

Brahim Gasbaoui¹ and Abdelfatah Nasri²

¹ Faculty of sciences and technology, Bechar University, gasbaoui_2009@yahoo.com

² Faculty of sciences and technology, Bechar University, nasriab1978@yahoo.fr

Abstract

The performance test of four different martial lead acid (Li-Acid), Nickel cadmium (Ni-Cd), lithium-ion (Li-Ion) and nickel metal hydride (NiMH) batteries for 4WD electric vehicle under several speeds variation constraints are presented in this paper. The battery materials model choice is a key item, and thanks to an increasing importance on vehicle range and performance, the Li-Acid, Ni-Cd, Li-Ion and NiMH batteries could become a viable candidate that's our proposal battery model in the present work, in this way the present paper show a novel strategy of 4WD electrical vehicle power electronics studies when the current battery take into account the impact of the direct torque based space vector modulation technique (DTC-SVM) in the several speed variations using the primitive battery SOC of 75 % state. The speed of four wheels is calculated independently during the turning with the electronic differential system computations which distributes torque and power to each in-wheel motor according to the requirements, adapts the speed of each motor to the driving conditions This paper focuses lead acid, Lithium-ion and NiMH Batteries controlled by Buck Boost DC-DC converter power supply for EV. The performances of the proposed strategy controller give a satisfactory simulation results. The proposed control law increases the utility EV autonomous under several roads topologies.

Keywords

4WD, lead acid, lithium-ion battery, SOC, nickel metal hydride.

1. INTRODUCTION

The principal constraints in vehicle design for transportation are the development of a non-polluting high safety and comfortable vehicle. Taking into account these constraints, our interest has been focused on the 4WD electrical vehicle, with independent driving wheel-motor at the front and with classical motors on the rear drive shaft [Wang et al., 2011]. This configuration is a conceivable solution, the pollution of this vehicle is strongly decreased and electric traction gives the possibility to achieve accurate and quick control of the distribution torque. Torque control can be ensured by the inverter, so this vehicle does not require a mechanical differential gear or gearbox [Wang et al., 2008]. One of the main issues in the design of this vehicle (without mechanical differential) is to assume the car stability. During normal driving condition, all drive wheel system requires a symmetrical distribution of torque in the both sides In recent years, due to problems like the energy crisis and environmental pollution, the Electric Vehicle (EV) has been researched and developed more and more extensively. Currently, most EVs are driven by two front wheels or two rear wheels. Considering some efficiency and

space restrictions on the vehicle, people have paid more and more attention in recent years to four-wheel drive vehicles employing the IM in-wheel motor.

Battery technology is one of most important areas of research pertaining to the reliability and commercial popularity of this alternative form of transportation. The battery forms a very crucial component of the drive train [Hori et al., 1998]. It provides the desired electric power to the traction motor in accordance with the driver's requirement. The battery properties widely vary with the chemistry. The battery should be capable of storing sufficient energy, offer high energy efficiency, high current discharge, and good charge acceptance from regenerative braking, high cycle time and calendar life and abuse tolerant capability. It should also meet the necessary temperature and safety requisites. Although many different types of energy storage technologies are under development, batteries are currently used as the main source of electric power in the EV. The three main battery chemistries that find application in the automotive industry are:

- Lead-Acid Battery
- Nickel Metal Hydride Battery
- Lithium-ion Battery [Scrosati et al., 2010]

The basic constructional feature of a lead acid battery as presented in the encyclopedia of alternative energy and sustainable living. The typical lead acid battery has a cell potential of 2.1 V, gravimetric en-

ergy of 35-50 Wh/kg and volumetric energy of 100 Wh/L. The most important constraint of the lead acid battery is its need for regular maintenance. This occurs when the battery is stored for a long period of time. Recent developments have diminished this backlog to an extent where they now can be used for low power hybrid electric vehicles (HEV) and EV. A major reason for the shortened life in lead acid batteries is sulphation. The electrolyte had been immobilized by using absorbent glass mat of highly porous microfiber construction and gelled electrolyte.

Nickel metal hydride (NiMH) batteries have dominated the automotive application since 1990's due to their overall performance and best available combination of energy and power densities, thermal performance and cycle life [Salman et al., 2005]. They do not need maintenance, require simple and inexpensive charging and electronic control and are made of environmentally acceptable recyclable materials. The capacity of NiMH cell is relatively high but its cell potential is 1.35 V [Nelson et al., 2000]. The gravimetric energy density is about 95 Wh/kg and volumetric energy is about 350 Wh/L. State of charge (SOC) symbols the residual capacity of battery and it written as the percent of residual capacity by nominal capacity the estimation of SOC of Lithium-ion battery is a key point of energy management system in EV. The accurate battery SOC monitor and control maintain battery's optimum potential and extend its life [Xia et al., 2006]. The aim of this paper is tested the performance of different batteries materials for the future 4WD electric vehicle.

2. ELECTRIC VEHICLE DESCRIPTION

According to Figure 1 the opposition forces acting to the vehicle motion are: the rolling resistance force due to the friction of the vehicle tires on the road; the aerodynamic drag force F_{aero} caused by the friction on the body moving through the air; and the climbing force F_{slope} that depends on the road slope [Wu et al., 2008].

The total resistive force is equal to F_r and is the sum of the resistance forces, as in (1) [Gasbaoui et al, 2011].

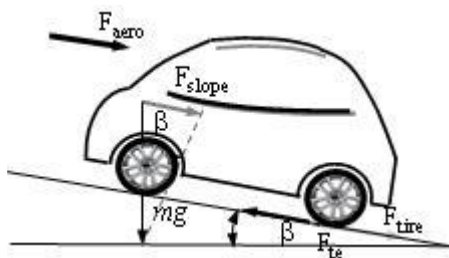


Fig. 1 The forces acting on a vehicle moving along a slope

$$F_r = A_f C_d \frac{\rho_a v^2}{2} + f_r M_v g \cos \beta + M_v g \sin \beta \quad (1)$$

aerodynamic resistance
rolling resistance
road slope

Where M_v is the total masse of vehicle is the tire radius, f_r is the rolling resistance force constant, g the gravity acceleration, ρ_{air} is Air density, C_d is the aerodynamic drag coefficient, A_f is the frontal surface area of the vehicle, v is the vehicle speed, β is the road slope angle. Values for these parameters are shown in Table 1.

Table 1 Parameters of the electric vehicle model

r	0.32 m	A_f	2.60 m ²
m	1300 Kg	C_d	0.32
f_r	0.01	ρ_{air}	1.2 Kg/m ³

The vehicle considered in this work is four in wheels motor EV destined to urban transportation. Two induction motors are coupled in each of the rear and front wheels. The energy source of the electric motors comes from the deferent's battery materials (the Li-Acid, Ni-Cd, Li-Ion and NiMH) controller by Buck boost DC-DC converter .The propulsion and control system schema of the EV is shown in Figure 4.

The differential electronics gives the reference speed as it show in Figure 5.

3. BOOST DC-DC CONVERTER FOR ELECTRIC VEHICLE

DC-DC Buck boosts converters find applications in places where battery charging, regenerative braking, and backup power are required. The power flow in a bidirectional converter is usually from a low voltage end such as battery or a super capacitor to a high voltage side and is referred to as boost operation [Chil et al., 2006]. Figure 11 show the electric vehicle propulsion chain using an DC-DC Buck boosts converters.

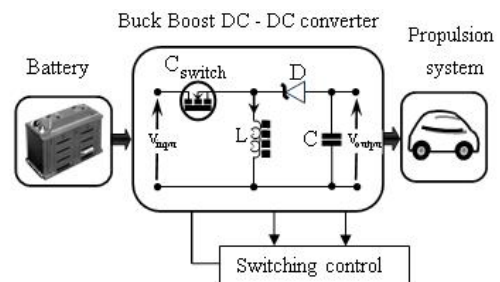


Fig. 2 The buck boost DC-DC converter control strategy scheme

4. DIRECT TORQUE CONTROL STRATEGY BASED SPACE VECTOR MODULATION (SVM-DTC)

With the development of microprocessors and DSP techniques, the SVM technique has become one of the most important PWM methods for Voltage Source Inverter (VSI) since it gives a large linear control range, less harmonic distortion, fast transient response, and simple digital implementation [Habetler et al., 1992]. The induction motor stator flux can be estimated by

$$\varphi_{ds} = \int_0^t (V_{ds} - R_s i_{ds}) dt \quad (2)$$

$$\varphi_{qs} = \int_0^t (V_{qs} - R_s i_{qs}) dt \quad (3)$$

$$|\varphi_s| = \sqrt{\varphi_{ds}^2 + \varphi_{qs}^2} \quad (4)$$

$$\varphi_s = \tan^{-1} \left(\frac{\varphi_{qs}}{\varphi_{ds}} \right) \quad (5)$$

And electromagnetic torque T_{em} can be calculated by:

$$T_{em} = \frac{3}{2} p (\varphi_{ds} i_{qs} - \varphi_{qs} i_{ds}) \quad (6)$$

The SVM principle is based on the switching between two adjacent active vectors and two zero vectors dur-

ing one switching period. It uses the space vector concept to compute the duty cycle of the switches. Figure 5 shows a scheme of a three-phase two-level inverter with a star-connection load.

5. SIMULATION RESULTS

In order to analyze the driving wheel system behaviour, Simulations were carried using the model of Figure 4. The following results were simulated in MATLAB and its divided in two phases. The first one deal with the test of the EV performances controlled with DTC strategy under several topology variation in the other hand we show the impact of this controller on vehicle power electronics performances. Only the front right motor simulations are shown. The assumption that the initialized lithium-ion battery SOC is equal to 75 % during trajectories .

5.1 Direct torque control scheme with space vector modulation

The topology studied in this present work consists of four phases: the first one is the beginning phase's with speed of 80 Km/h in straight road topology, the second phases present sloped road effect, the third phases present the curved road with the same speed, finally the 4WD moving up the descent road of 10 % under 80 Km/h, the specified road topology is shown in Figure 5, when the speed road constraints are described in the Table 2.

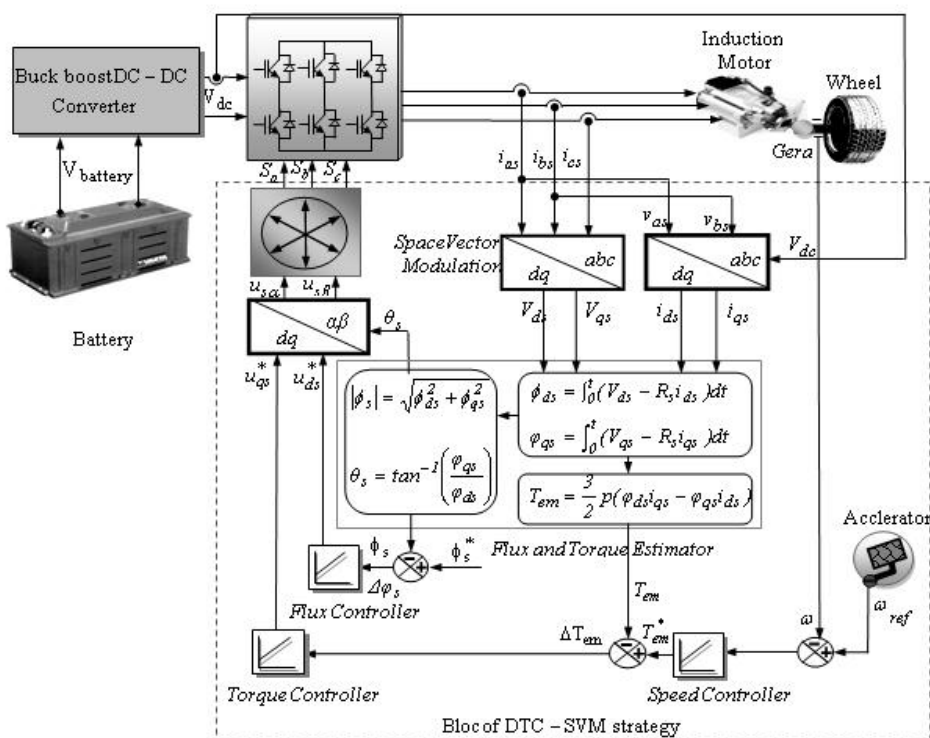


Fig. 3 Bloc diagram for DTC strategy based space vector modulation

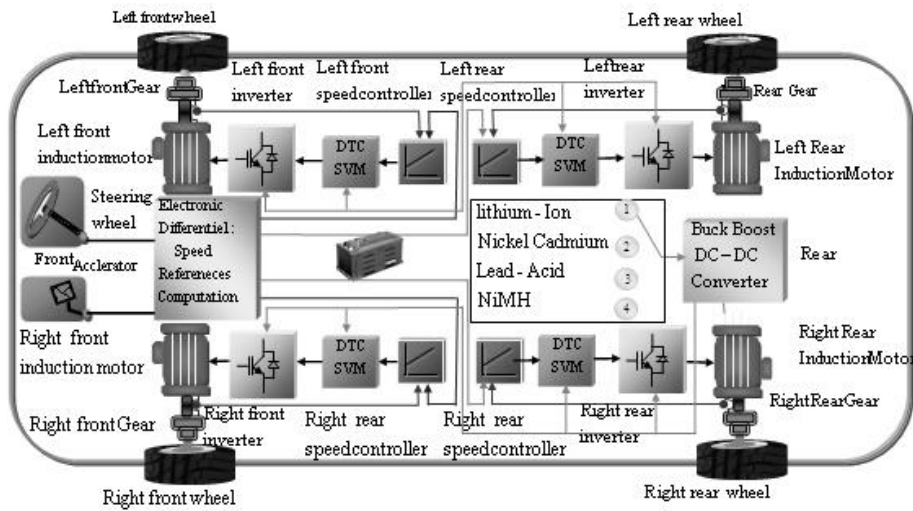


Fig. 4 The driving wheels control system

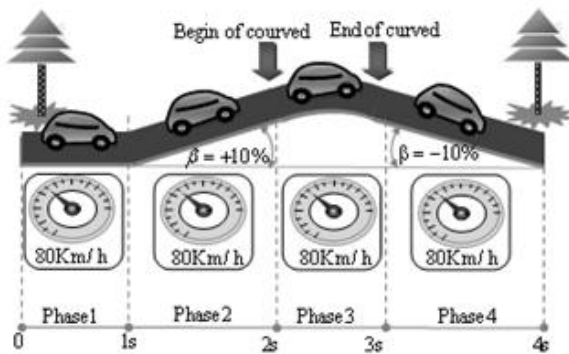


Fig. 5 The chosen road topology of tests

Table 2 The driving road topology description

Phases	Event information	Vehicle speed [km/h]
Phase 1	beginning	80
Phase 2	Sloped road of 10 %	80
Phase 3	Curved road	80
Phase 4	Descente slope of 10 %	80

Referred to Figure 6 At $t = 1$ s, the 4WD electric vehicle are driving in straight road, this test explain the sloped effect on the 4WD. The driving wheels linear speeds stay the same and the road drop does not influence the DTC-SVM of each wheels. At $t = 2$ s the vehicle driver turns the steering wheel on a curved road at the right side with speed of 80 km/h, the assumption is that the four motors are not disturbed. In this case the front and rear driving wheels follow different paths, and they turn in the same direction but with different speeds. The electronic differential acts on the four motor speeds by decreasing the speed of the driv-

ing wheel on the right side situated inside the curve, and on the other hand by increasing the wheel motor speed in the external side of the curve. The behaviours of these speeds are given in Figure 6. At $t = 3$ s the vehicle situated in the second curve but in the left side, the electronic differential compute the novel steering wheels speeds references in order to stabilize the vehicle inside the curve. The battery initial SOC of 75 % for Li-Acid, Ni-Cd, Li-Ion and NiMH is respected. In this case the driving wheels follow the same path with no overshoot and without error which can be justified with the good electronic differential act coupled with DTC-SVM performances. At $t = 3$ s clarifies the effect of the descent slope on the 4WD electric vehicle moving on straight road. The linear speed responses are illustrated in Figure 6. The 4WD electric vehicle speeds are the same for each battery materials.

Figure 7 and Table 3, explains the variation of phase current and electromagnetic torque respectively. In the first step and to reach 80 km/h The 4WD demand

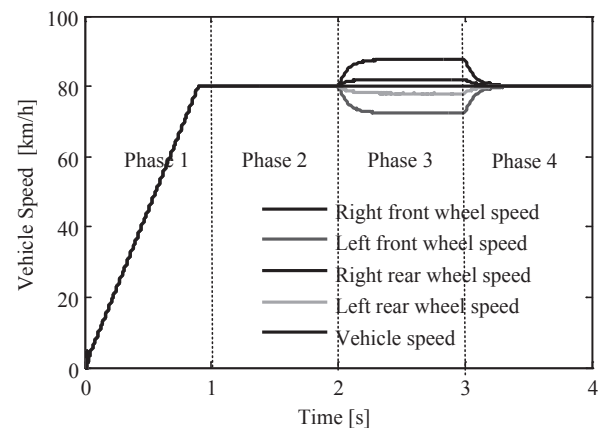


Fig. 6 Variation of vehicle speeds in different scenarios

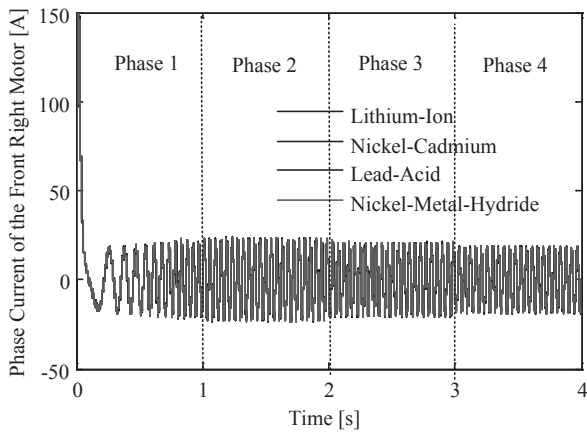


Fig. 7 Variation of phase current of the front motor right in different phases

Table 3 Values of phase current electromagnetic torque of the right motor in different phases

Phases	1	2	3	4
Current of the front motor right [A]	22.40	23.25	20.85	18.77
Electromagnetic torque of front motor right [N.m]	39.14	53.82	42.93	33.07

a current of 22.410 A for each motors which explained with electromagnetic torque of 39,14 N.m. The second phase explains the effect of the sloped road the electromagnetic torque increase and the current demand undergo double of the current braking phases, The four motor induction develops more and more electromagnetic torque for vanquish the slop. They develops approximately 53.82 N.m each one. The current demand increases and the vehicle can pass the slope easily. The linear speeds of the four induction motors stay the same and the road drop does not influence

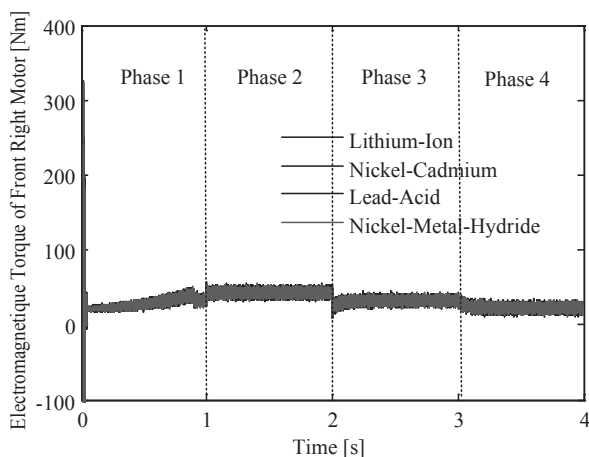


Fig. 8 Variation of electromagnetic torque of the front motor right in different phases

the torque control of each wheels In the curved road the current and electromagnetic torque demand are computed using the electronic differential process according to the driver decision by means that the speed reference of each wheels is given by the electronic differential computations witch convert the braking angle in the curve on linear speeds .The Figure 8 show the electromagnetic torque of the front right motor for each kind of battery materials. The last phases illustrate the deceleration effect. The results are listed in Table 3.

According to the formula (1) and Table. 4 The variation of vehicle torques in different cases as shown in Figure 9. The vehicle torque develops 127.73 N.m in the first phase. In the second phase the electromagnetic torque go up 127.60 N.m to 168.40 N.m that present amount of 42.90 % of the total nominal motor torque 392.40 Nm. This variation makes clear the slop torque effect's on the traction chain. In the third phases the propulsion system develops the necessary efforts to pass the curved road. In the last case a great decreases for electromagnetic torque around 50 % of the slope torque (deceleration phase's when the battery is in the recharge state), the resistive torque of present 22.88 % of globally nominal motor torque. The result prove that the traction chain under slope constraint develop the double effort comparing with the inverse slope case by means that the vehicle needs the half of its

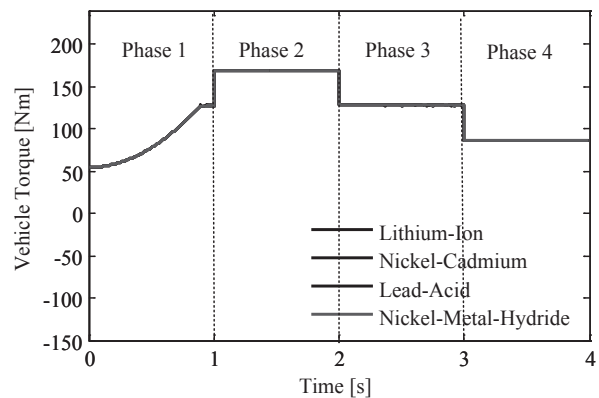


Fig. 9 Variation of vehicle resistive torque in different phases

Table 4 Variation of vehicle torque in different phases

Phases	1	2	3	4
the Vehicle resistive torque [N.m]	127.6	168.40	127.60	86.81
the globally vehicle resistive torque Percent compared with nominal motor torque of 392.46 Nm	32.51	42.90	32.51	22.88

energy in the deceleration phase's compared with the acceleration one's as it specified in Table 3 and Figure 9.

5.2 Power electronics

The Li-Acid, Ni-Cd, Li-Ion and NiMH batteries must be able to supply sufficient power to the EV in accelerating and decelerating phase, which means that the peak power of the batteries supply must be greater than or at least equal to the peak power of the four electric motors. The battery must store sufficient energy to maintain their SOC at a reasonable level during driving, Figure 10, describe the changes in the battery storage power in different speed references.

It is interesting to describe the power distribution in the electrical traction under several speed references as it described in Figures 10 and 11. The battery provides about 9.12 Kw in the first phase in order to reach the electronic differential reference speed of 80 Km/h. In the second phase (phase 2: sloped phase's) the demanded power battery increase and it present amount of 41.80 % of the globally nominal power battery (31 Kw). In the curved road the battery produced power equal to 9.83 Kw for vanquish this situation .

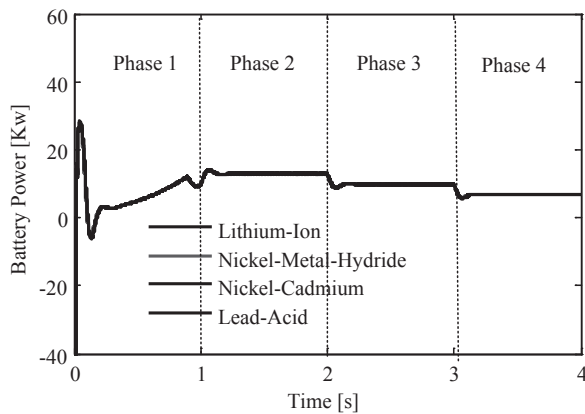


Fig. 10 Variation of batteries power in different phases

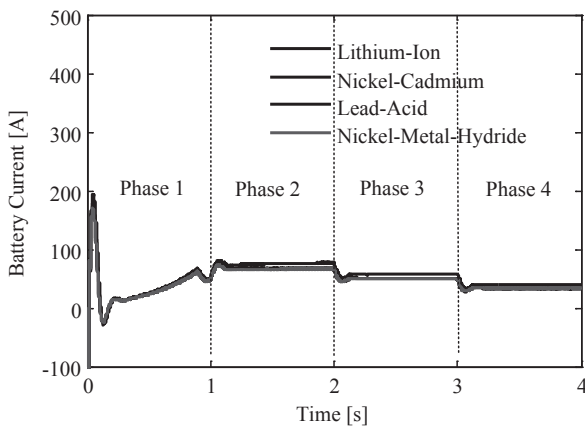


Fig. 11 Variation of batteries current during trajectory

Table 5 Variation of battery power in different trajectory phases

Phase	1	2	3	4
consumed Battery power [Kw]	9.12	12.96	9.83	6.80
Percentage of the battery power compared with battery power [31 Kw]	29.41	41.80	31.70	21.93

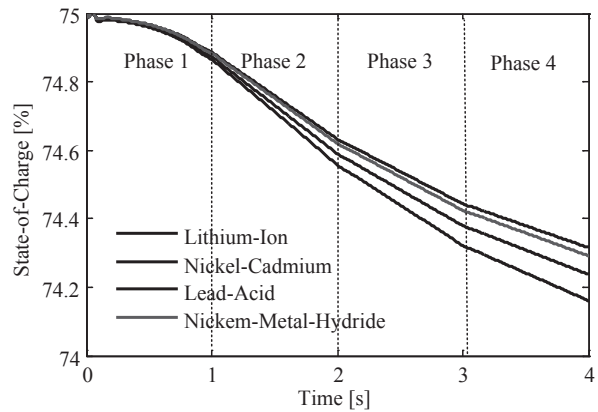


Fig. 12 Battery efficiency versus state-of-charge

Table 6 Evaluation of SOC [%] in the different phases for Li-Acid, Ni-Cd, Li-Ion and NiMH batteries

		SOC begin [%]	SOC end [%]	SOC diff [%]
Phase 1	Li_Ion	75	74.87	0.13
	Ni-MH	75	74.87	0.11
	L-Acid	75	74.87	0.13
	Ni-Cd	75	74.89	0.11
Phase 2	Li_Ion	74.87	74.59	0.28
	Ni-MH	74.88	74.62	0.26
	L-Acid	74.87	74.56	0.31
	Ni-Cd	74.89	74.63	0.26
Phase 3	Li_Ion	74.59	74.38	0.21
	Ni-MH	74.62	74.43	0.19
	L-Acid	74.56	74.32	0.24
	Ni-Cd	74.63	74.44	0.19
Phase 4	Li_Ion	74.38	74.24	0.14
	Ni-MH	74.43	74.29	0.14
	L-Acid	74.32	74.16	0.16
	Ni-Cd	74.44	74.32	0.12

The battery produced power depend only on the electronic differential consign by means the acceleration/ deceleration driver state which can be explained by evaluation of the battery SOC for ache batteries of Figure 12.

Figure 15 explains how SOC in the four batteries materials changes during the driving cycle; it seems that the SOC decreases rapidly at second phases (sloped road effect's), by means that the SOC range's between 74.88 % to 74.62 % of Ni-MH battery. During all cycle's phases from beginning at the end cycles it was initialized to 75 % at the beginning of the simulation. Figure 13 clarify a slight improvement of Ni-cadmium battery compared with Ni-MH battery.



Fig. 13 Comparative study of SOC for different batteries during all trajectories

Figure 14 investigates the variation of state of charge function of time delay. The relationship between SOC and left time of each Li-Ion materials are defined by the flowing linear fitting formula:

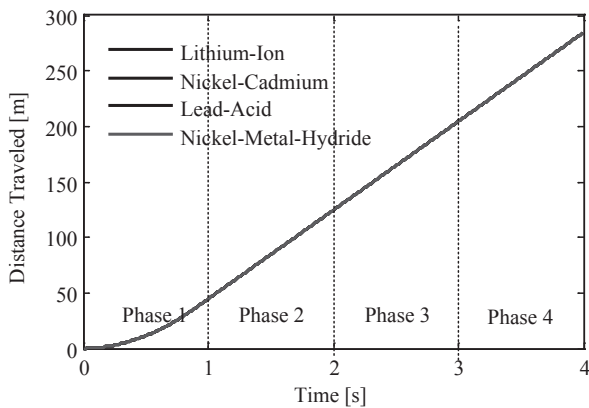


Fig. 14 Variations of the travelled distance in different cases

$$SOC[\%] = -4.8e-5t^5 - 0.0077t^4 + 0.081t^3 - 0.26t^2 + 0.072t - 75 \tag{7}$$

We can define the relationship between the state of charge for Ni-MH battery and the traveled distance in each phases by the linear fitting formula:

$$d_{trveled} = -1.2e2SOC^5 - 4.3e4SOC^4 + 6.5e6SOC^3 + 4.9e8SOC^2 + 1.8e10SOC - 2.7e11 \tag{8}$$

This power is controlled by the Buck Boost DC-DC converter current and distribute accurately for four phases. Figure 15 show the buck boost DC-DC converter robustness under several speed cycles. The buck boost converter is not only a robust converter which ensure the power voltage transmission but also a good battery recharger in deceleration state that help to perfect the vehicle autonomous with no voltage ripple.

Table 7 The relationship between the traction chain power electronics characteristics and the distance traveled in different phases for each battery materials

Phase 1			
Li_Ion	44.38	0.13	9.12
Ni-MH	44.38	0.12	12.96
L-Acid	44.38	0.13	9.93
Ni-Cd	44.38	0.11	6.80
Phase 2			
Li_Ion	79.92	0.28	9.12
Ni-MH	79.92	0.26	12.96
L-Acid	79.92	0.31	9.93
Ni-Cd	79.92	0.26	6.80
Phase 3			
Li_Ion	79.92	0.21	9.12
Ni-MH	79.92	0.19	12.96
L-Acid	79.92	0.24	9.93
Ni-Cd	79.92	0.19	6.80
Phase 4			
Li_Ion	79.92	0.14	9.12
Ni-MH	79.92	0.14	12.96
L-Acid	79.92	0.16	9.93
Ni-Cd	79.92	0.12	6.80
Total distance traveled [m]			
284.14			

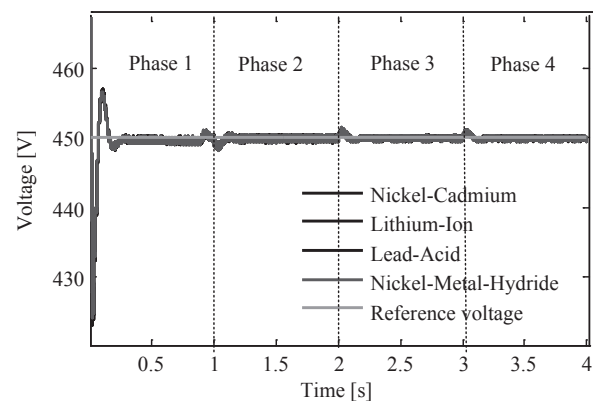


Fig. 15 Buck Boost DC-DC converter behavior under several speed variations.

6. CONCLUSION

The power propulsion system studied in this paper has demonstrated that the Nickel metal hydride battery behavior controlled by buck boost DC-DC converter for utility 4WD electric vehicle can be improved using direct torque control strategy based on space vector modulation when the battery developed power depend on the speed reference of the driver and road topologies. The several speed variations do not affect the performances of the Nickel metal hydride battery and the control strategy gives good dynamic characteristics of the EV propulsion system. This paper proposes novel fitting formulas which give the relationship between the SOC and distance travelled and others formulas that give more efficiency to different propulsion systems paths. According to the obtained results in different road scenarios and comparing with other battery sources, it can be concluded that Nickel metal hydride battery became an energy source candidate for the next future 4WD electric vehicle moving in mountainous regions.

References

- Chill, H., and L. Lin, A bidirectional DC-DC converter for fuel cell electric vehicle driving system, *IEEE Transactions on Power Electronics*, Vol. 21, 950-958, 2006.
- Gasbaoui, B., A., Chaker, A. Laoufi, Multi-input multi-output fuzzy logic controller for utility electric vehicle Drive, *Archives of Electrical Engineering*, Vol. 60, No. 3, 239-256, 2011.
- Habetler, T., F. Profumo, M. Pastorelli, L. Tolbert, Direct torque control of induction machines using space vector modulation, *IEEE Transaction on Industry Applications*, Vol. 28, No. 5, 1045-1053, 1992.
- Hori, Y., Y. Toyoda, and Y. Tsuruoka, Traction control of electric vehicle: Basic experimental results using the test EV "UOT Electric March", *IEEE Transactions on Industry Applications*, Vol. 34, No. 5, 1131-1138, 1998.
- Nelson, R. F., Power requirements for battery in HEVs, *Journal of Power Sources*, Vol. 91, 2-26, 2000.
- Salman, M., M. Chang, and J. Chen, Predictive energy management strategies for hybrid vehicles, *Proceedings of IEEE VPPC*, 21-25, 2005.
- Scrosati, B., and J. Garche, Lithium batteries: Status, prospects and future, *Journal of Power Sources*, Vol. 195, 2419-2430, 2010.
- Villevieille, C., F. Robert, P. Taberna, L. Bazin, P. Simon, and L. Monconduit, The good reactivity of lithium with nanostructured copper phosphide, *Journal of Material Chemistry*, Vol. 18, 5956-5960, 2008.
- Xia, C., and Y. Guo, Implementation of a bi-directional DC/DC converter in the electric vehicle, *Journal of Power Electronics*, Vol. 40, No. 1, 70-72, 2006.
- Wang, J., Q. Wang, and L. Jin, Modeling and simulation studies on differential drive assisted steering for EV with four-wheel-independent-drive, *Proceedings of the 4th IEEE vehicle power and propulsion conference*, 2008.
- Wang, J., Q. Wang, L. Jin, and C. Song, Independent wheel torque control of 4WD electric vehicle for differential drive assisted steering, *Mechatronics*, Vol. 21, 63-76, 2011.
- Wu, F., and T. Yeh, A control strategy for an electrical vehicle using two in-wheel motors and steering mechanism. *Proceedings of AVEC*, 796-801, 2008.

(Received December 25, 2011; accepted February 13, 2011)